Available online at www.sciencedirect.com
ScienceDirect
Journal of Organometallic Chemistry 692 (2007) 1834–1844
Journal of Organometallic Chemistry
www.elsevier.com/locate/jorganchem

Ferrocenylpyrazole—A versatile building block for hydrogen-bonded organometallic supramolecular assemblies

Tomoyuki Mochida [a,b,*], Fumiko Shimizu [a], Hirotaka Shimizu [a], Kazuya Okazawa [a], Fuminori Sato [c], Daisuke Kuwahara [c]

[a] Department of Chemistry, Faculty of Science, Toho University, Miyama, Funabashi, Chiba 274-8510, Japan
[b] Research Center for Materials with Integrated Properties, c/o Faculty of Science, Toho University, Japan
[c] The University of Electro-Communications, Chofu, Tokyo 182-8585, Japan

Received 1 September 2006; received in revised form 7 November 2006; accepted 7 November 2006
Available online 16 November 2006

Abstract

The crystal architectures of 5-ferrocenylpyrazole (**1**) and its metal complexes were investigated. Compound **1** can form non-solvated and chloroform-solvated crystals. In both cases, **1** forms a zigzag one-dimensional architecture via NH···N hydrogen bonds. The hydrogen bond exhibits a twofold disorder, which was shown to be static by solid-state ^{13}C NMR. In the solvated crystal, the chloroform is released at 415 K, associated with melting of the crystal. The reaction of **1** with metal salts provided metal-centered ferrocenyl clusters $[Zn(NO_3)_2(\mathbf{1})_4]$ (**4**), $[Co(NO_3)_2(\mathbf{1})_4]$ (**5**), $[CoCl_2(\mathbf{1})_4]$ (**6**), $[Zn(NCS)_2(\mathbf{1})_2]$ (**7**), *cis*-$[Pt(NH_3)_2(\mathbf{1})_2](PF_6)_2$ (**8**), and *trans*-$[Pt(NH_3)_2(\mathbf{1})_4](PF_6)_2$ (**9**). In all of these complexes, **1** acts as a monodentate ligand. In **4**, **5**, and **7**, the multinuclear units are joined via hydrogen bonds to form supramolecular chains. Two polymorphs were found for the crystals of **4**. Both are composed of the same hydrogen-bonded chains, but their arrangements are different. 5-Ferrocenyl-1-tritylpyrazole (**2**) and 4-ferrocenyl-1-methylpyrazole (**3**) were also crystallographically characterized.

Keywords: Crystal structure; Hydrogen bond; Pyrazole; Ferrocene; Metal complex

1. Introduction

Various organometallic supramolecular assemblies have been reported to date [1–3]. In the construction of supramolecular assemblies, hydrogen bonds and coordination bonds play essential roles. Our approach toward the study of organometallic supermolecules is to introduce heteroaryl substituents into ferrocenes, which has led to the design of versatile ligands such as 5-ferrocenylpyrimidine (FcPM) [4] and relevant ligands [5]. FcPM gives various assembled structures when combined with transition metal salts, and its combination with hydrogen-bond donors leads to hydrogen-bonded supermolecules with various dimensions [4d]. We also prepared ferrocenyl tetrazoles and triazoles, which exhibit one-dimensional crystal architecture based on weak N···HC hydrogen bonds [6]. In this study, to realize the synergy of hydrogen bonds and coordination bonds in an organometallic molecular assembly, we designed 5-ferrocenylpyrazole (FcPz, **1**). Pyrazole derivatives form intriguing hydrogen-bonded assemblies, such as chains, cyclic tetramers, trimers, and dimers (Fig. 1a), and they often show disorder with respect to their NH protons [7]. The hydrogen bond in pyrazoles has drawn attention in terms of intermolecular proton transfer [8]. Furthermore, pyrazole derivatives are versatile ligands [9] that can act as monodentate ligands in their neutral form (Fig. 1a) and as bidentate bridging ligands in the form of pyrazolate

* Corresponding author. Address: Department of Chemistry, Faculty of Science, Toho University, Miyama, Funabashi, Chiba 274-8510, Japan. Tel./fax: +81 47 472 4406.
E-mail address: mochida@chem.sci.toho-u.ac.jp (T. Mochida).

0022-328X/$ - see front matter © 2006 Elsevier B.V. All rights reserved.
doi:10.1016/j.jorganchem.2006.11.011

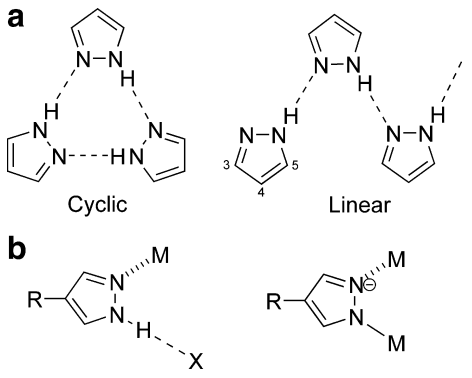

Fig. 1. (a) Hydrogen bonding modes in pyrazoles and (b) assembly modes of metal complexes with pyrazoles.

anions (Fig. 1b). The NH group in the neutral form can form hydrogen bonds. For these reasons, **1** is an interesting molecule with respect to the design of organometallic supermolecules. Similar ligands 3-ferrocenylpyrazole [10] and ferrocenylmethylpyrazole [11] have previously been investigated, and intriguing metallocene ligands exhibiting both hydrogen bonding and metal complexation [12] are known to exist. Here we report the preparation and crystal architecture of **1** and its metal complexes.

2. Results and discussion

2.1. Preparation and properties of *1* and its metal complexes

5-Ferrocenylpyrazole (**1**) was obtained by hydrolysis of 4-ferrocenyl-1-tritylpyrazole (**2**), which was prepared by Negishi coupling [4a,13] of chlorozincated ferrocene and iodotritylpyrazole (Scheme 1). Acetic acid was used for hydrolysis to avoid oxidation of the ferrocenyl moiety. We also prepared 4-ferrocenyl-1-methylpyrazole (**3**) by methylation of **1**. Recrystallization of **1** from acetonitrile produced non-solvated crystals, while recrystallization from chloroform produced solvated crystals ($\mathbf{1}\cdot 0.5CHCl_3$), both of which were crystallographically characterized. To examine the solvent desorption process from the solvated crystal, we performed thermogravimetric (TG) analysis of both crystal types. The TG trace of the non-solvated crystal showed a gradual decrease above 510 K, which corresponds to degradation. The melting point of this crystal was determined to be 431.7 K by differential scanning calorimetry ($\Delta H = 24.2$ kJ mol^{-1}). On the other hand, the TG trace of the chloroform-solvated crystal exhibited a sudden weight loss of 10% at 415 K, and with further increasing temperature, it showed a gradual decrease above 520 K. This observation suggests that the chloroform in the solvated crystals is suddenly released at 415 K, associated with melting of the crystal lattice. Thus, the guest molecule is held in the crystal above its boiling point of 335 K.

Reaction of **1** with zinc and cobalt salts provided metal-centered ferrocenyl clusters (Scheme 2), $[Zn(NO_3)_2(\mathbf{1})_4]$ (**4**), $[Co(NO_3)_2(\mathbf{1})_4]$ (**5**), $[CoCl_2(\mathbf{1})_4]$ (**6**), and $[Zn(NCS)_2(\mathbf{1})_2]$ (**7**), which were crystallographically characterized. Reaction of **1** with platinum salts in aqueous media produced *cis*-$[Pt(NH_3)_2(\mathbf{1})_2](PF_6)_2$ (**8**) and *trans*-$[Pt(NH_3)_2(\mathbf{1})_4](PF_6)_2$ (**9**) in high yields. Compound **1** acted as a monodentate ligand in all of these complexes.

The redox potentials of **1**, **2**, **8**, and **9** were measured in acetonitrile by cyclic voltammetry. Compounds **1** and **2** exhibited quasi-reversible waves at $E_{1/2} = -0.04$ and -0.03 V, respectively (vs. Cp_2Fe/Cp_2Fe^+), which correspond to the redox potentials of the ferrocenyl moieties. This is much lower than those of other heteroarylferrocenes, e.g. 0.14, 0.21, and 0.27 V for ferrocenylpyrimidine (FcPM), ferrocenyltetrazole, and ferrocenyltriazole, respectively [4e,6], which is consistent with the substituent effect [14]. Platinum complexes **8** and **9** each showed one redox wave, at $E_{1/2} = 0.21$ and 0.22 V, respectively, which indicates that no electrochemical communication occurs between the ferrocenyl groups through the metal center. Metal complexation generally raises the redox potential of the ligand [4e,15]. Despite the lower redox potential of **1**, the redox potentials of its platinum complexes were comparable to those of FcPM complexes ($E_{1/2} = 0.20$–0.21 V) [4e]. This result is probably ascribable to the higher electron donating ability of **1** over FcPM.

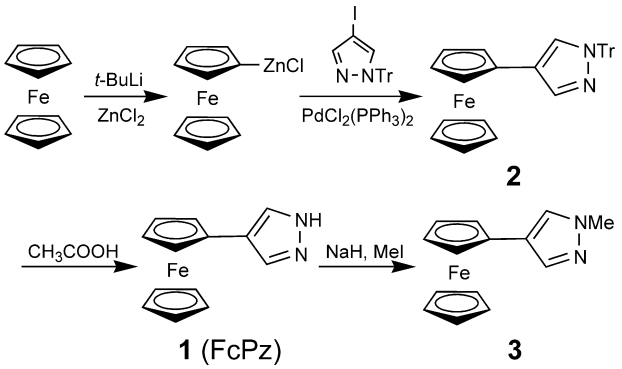

Scheme 1.

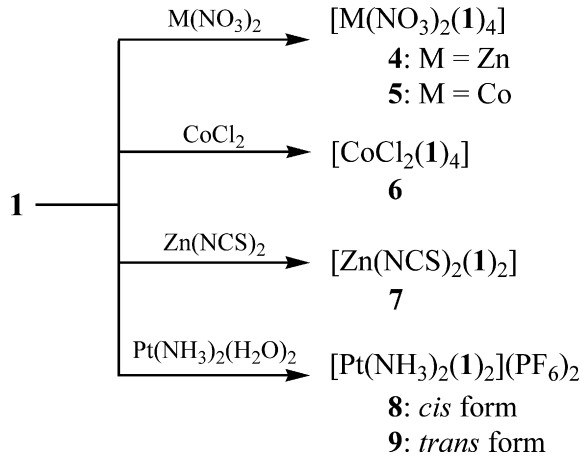

Scheme 2.

Table 1
Hydrogen bond lengths (Å) in **1** and its chloroform solvate

	N(1)···N(1)	N(2)···N(3)	N(4)···N(4)
1	2.899(3)	2.879(3)	2.888(3)
1 · 0.5$CHCl_3$	2.865(7)	2.857(7)	2.940(7)

2.2. Structure and hydrogen bonding in *1* and its chloroform solvate

The non-solvated and chloroform-solvated crystals of **1** are both composed of chains of **1** connected via NH···N hydrogen bonds. These crystals exhibit disorder with respect to their NH protons, as shown below. The hydrogen bond distances are listed in Table 1; they are within the usual range of N···N hydrogen-bond distances (2.8–3.2 Å) found for pyrazole chain compounds [7], but are rather shorter than average.

Packing diagrams of each crystal form, projected along the chain direction (*a*-axes), are shown in Fig. 2. In the solvated crystal, chloroform is accommodated in channels between the chains of **1** (Fig. 2b). The hydrogen-bonded chains in both crystal forms have an almost identical molecular arrangement. Fig. 3 shows the structure of the chain in the chloroform-solvated crystal. The chain is made up of two crystallographically independent molecules, A and B. The Cp–Py rings in **1** are almost coplanar. The chain consists of a repeating unit of –A–A–B–B–, with inversion centers between A–A and also between B–B. Therefore, the pyrazole rings of the A molecules related by the inversion center are coplanar, which also holds for the B molecules. The dihedral angle between the pyrazole rings of molecules A and B is 74.4(3)° in the solvated crystal, and 82.6(1)° in the non-solvated crystal. The inversion center also imposes symmetry on the intermolecular hydrogen-bond potentials between A–A and between B–B. Thus, the pyrazole NH protons are delocalized symmetrically over two sites, with an equal statistical occupancy at 0.5. The intramolecular bond lengths of the pyrazole moieties in both crystals are shown in Fig. 4. The pyrazole rings show apparent C_{2v} symmetry, which is not crystallographically imposed, and no bond alternation was recognized. This is consistent with the symmetrical distribution of the hydrogen bond. Crystal structures of 4-ferrocenyl-1-tritylpyrazole (**2**) and 4-ferrocenyl-1-methylpyrazole (**3**) were also determined, and ORTEP drawings of the molecular structures of **2** and **3** were deposited as Supplementary materials. In these cases, clear bond alternation of the pyrazole ring was apparent (Fig. 4c and d). In these molecules, the Cp–Pyrazole planes are twisted by 29.8(3)° and 3.0(2)°, respectively.

The zig-zag hydrogen-bonded molecular arrangement, as well as its delocalization, is similar to that observed in 4-(1-adamantyl)pyrazole and other materials [16]. Proton

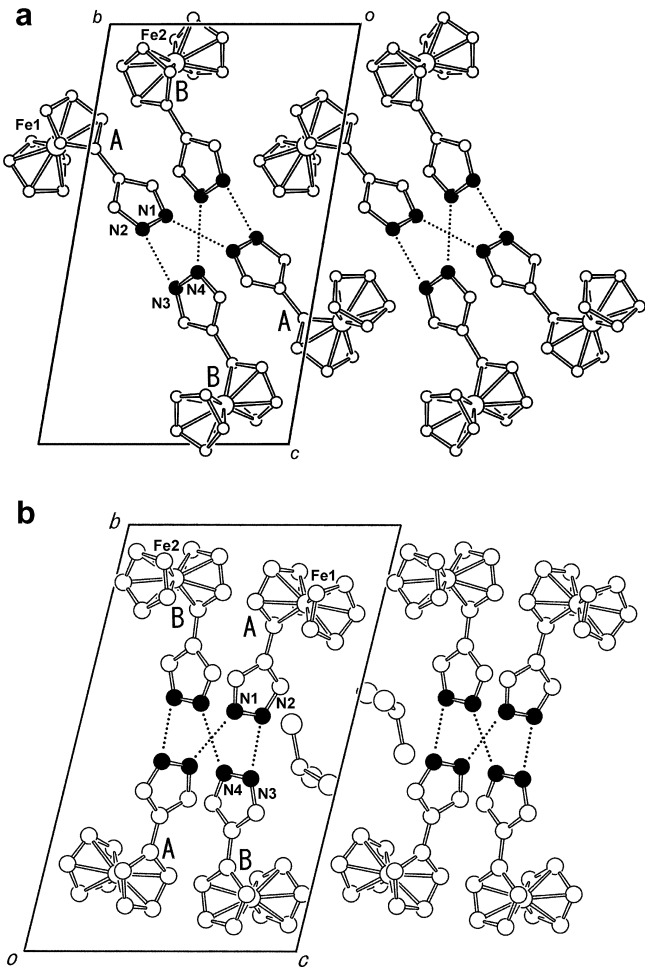

Fig. 2. Packing diagrams of (a) 5-ferrocenylpyrazole (**1**) and (b) its chloroform solvate. Symbols A and B denote crystallographically independent molecules. Dashed lines indicate hydrogen bonds. Hydrogen atoms are omitted for clarity.

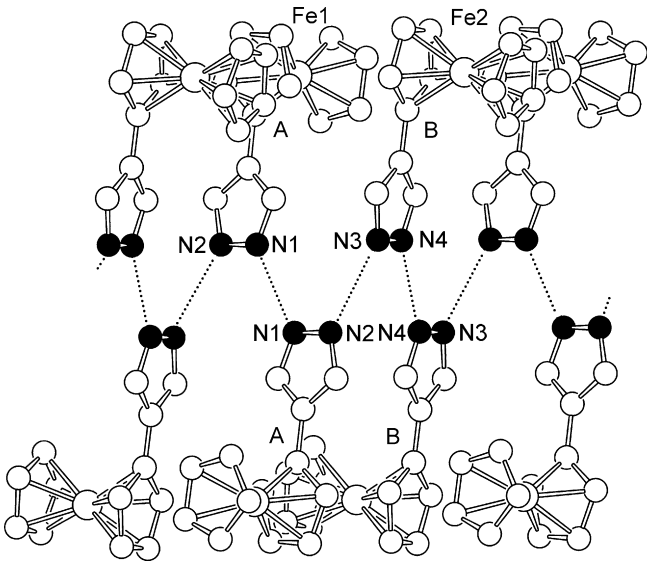

Fig. 3. Hydrogen-bonded one-dimensional zig-zag arrangement of 5-ferrocenylpyrazole (**1**) in the chloroform-solvated crystal. Dashed lines indicate hydrogen bonds. Symbols A and B denote crystallographically independent molecules. Hydrogen atoms are omitted for clarity.

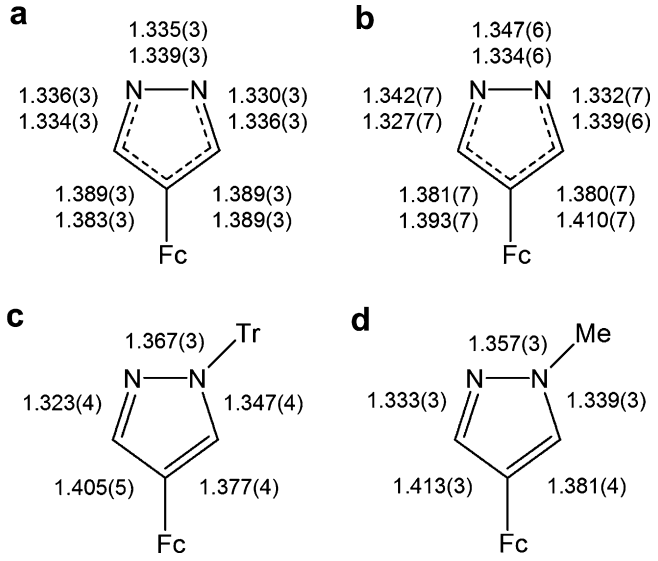

Fig. 4. Intramolecular bond lengths (Å) in (a) 5-ferrocenylpyrazole (**1**, non-solvated form), (b) 5-ferrocenylpyrazole (**1**, chloroform solvate), (c) 4-ferroceny-1-tritylpyrazole (**2**), and (d) 4-ferroceny-1-methylpyrazole (**3**).

Table 2
^{13}C NMR chemical shifts (δ, ppm) for **1** in the solid state

Assignment[a]	Chemical shifts[b] (T_1)
C3	136.7, 135.3(198)
C5	126.4, 123.8(179)
C4	120.4, 119.8(15)
C(C_5H_4)–Pz	78.8, 77.4(39, 65)
C(C_5H_5)	70.3, 69.7(9)
C(C_5H_4)–H	67.5, 56.6(39)

Values of T_1(s) are shown in parentheses.
[a] Positions of C3, C4, and C5 are shown in Fig. 1.
[b] Site splitting was observed.

transfer in one-dimensional hydrogen-bonded systems is of interest from the viewpoint of proton dynamics involving the mechanism of solitonic excitation [17]. In pyrazoles, the disordered hydrogen bond is considered to be dynamic only in some cyclic structures [9], but, interestingly, 4-(1-adamantyl)pyrazole exhibits an exchange process probably associated with molecular reorientation [16]. To investigate proton dynamics and molecular motion of **1** in the crystal, we performed ^{13}C CP/MAS NMR measurements on a polycrystalline sample of the non-solvated form. Dipolar dephasing experiments and ^{13}C spin–lattice relaxation time (T_1) measurements were also carried out. Chemical shifts of the peaks and their assignments are listed in Table 2. In the ^{13}C CP/MAS spectrum, signals for C3 and C5 (Fig. 1) appeared separately at around 135 and 125 ppm, which indicates that the disorder is static. The line shape was invariant between 190 and 353 K. T_1 was long (~200 s) for C3 and C5, which further supports the static nature of the disorder. A short T_1 (9 s) was observed for the C_5H_5 carbons, which suggests that the ring undergoes rotation at room temperature. Consistently with this, dipolar dephasing for the C_5H_5 carbons was not effective. No phase transitions were detected by DSC measurement between 100 and 460 K except at the melting point.

Table 3
N···O distances (Å) in hydrogen bonds in **4** and **5**

	Intramolecular	Intermolecular
4 (α-form)	2.862(2)	2.738(2)
4 (β-form)	2.86(1)	2.76(1)
5	2.848(3)	2.745(3)

Table 4
Selected bond lengths (Å) and angles (°) in **4**–**7**

4 (α-form)					
Zn(1)–N(1)	2.112(1)	Zn(1)–N(3)	2.132(1)	Zn(1)–O(1)	2.178(1)
N(1)–Zn(1)–N(3)	90.42(5)	N(1)–Zn(1)–O(1)	84.15(5)	N(3)–Zn(1)–O(1)	93.59(5)
Cp(Fe1)–Pz[a]	17.7(1)	Cp(Fe2)–Pz[a]	30.0(1)		
4 (β-form)					
Zn(1)–N(1)	2.135(6)	Zn(1)–N(3)	2.115(6)	Zn(1)–O(1)	2.182(5)
N(1)–Zn(1)–N(3)	90.6(2)	N(1)–Zn(1)–O(1)	83.6(2)	N(3)–Zn(1)–O(1)	93.1(2)
Cp(Fe1)–Pz[a]	13.5(3)	Cp(Fe2)–Pz[a]	26.6(6)		
5					
Co(1)–N(1)	2.108(2)	Co(1)–O(1)	2.152(2)	N(3)–Co(1)–O(1)	93.34(7)
Co(1)–N(3)	2.108(2)	N(1)–Co(1)–N(3)	90.54(8)	N(1)–Co(1)–O(1)	83.11(7)
Cp(Fe1)–Pz[a]	18.3(2)	Cp(Fe2)–Pz[a]	30.6(2)		
6					
Co(1)–N(1)	2.130(2)	Co(1)–Cl(1)	2.526(5)	N(3)–Co(1)–Cl(1)	90.44(5)
Co(1)–N(3)	2.118(2)	N(1)–Co(1)–N(3)	92.05(7)	N(1)–Co(1)–Cl(1)	87.99(5)
Cp(Fe1)–Pz[a]	17.0(2)	Cp(Fe2)–Pz[a]	13.9(2)		
7					
Zn(1)–N(1)	2.003(2)	Zn(1)–N(3)	1.937(2)	N(1)–Zn(1)–N(3)	103.68(8)
N(1)–Zn(1)–N(1)[b]	103.55(9)	N(3)–Zn(1)–N(3)[b]	112.4(1)	Cp–Pz[a]	17.5(1)

[a] Dihedral angle between the Cp and pyrazole rings.
[b] Symmetry code: $-x+1, y, -z+1/2$.

2.3. Structures of metal-centered ferrocenyl clusters 4–7

Compounds **4**–**7** are metal-centered ferrocenyl clusters in which **1** acts as a monodentate ligand. Three of these clusters (**4**–**6**) are centrosymmetric pentanuclear complexes, while **7** is a trinuclear complex. The ligand tends to form assembled structures in which coordination bonds and hydrogen bonds coexist. There are two crystallographically independent molecules in each unit in **4**–**6**, and one in **7**. Bond lengths around the metal atoms and Cp–Pz angles are listed in Table 4.

$[Zn(NO_3)_2(\mathbf{1})_4]$ (**4**) has two polymorphs, the α-form and the β-form. The molecular structure of the α-form is shown in Fig. 5a. The units form a chain structure via intermolecular NH···O hydrogen bonds (Fig. 5b). In the molecule, the Zn ion exhibits an octahedral coordination geometry, and the nitrate anions are at the axial positions. In the unit cell, intramolecular hydrogen bonds are formed between the NH hydrogens of two ligands and two nitrate anions [N(2)···O(2) distance: 2.862(2) Å] (Fig. 5a). The NH hydrogens of the other two ligands are involved in intermolecular hydrogen bonding with the nitrate oxygens of adjacent units [N(4)···O(3) distance: 2.738(2) Å], connecting the unit along the *a*-axis. The structure of the hydrogen-bonded chain in the β-form is almost the same. Hydrogen-bond lengths for both forms are comparable (Table 3).

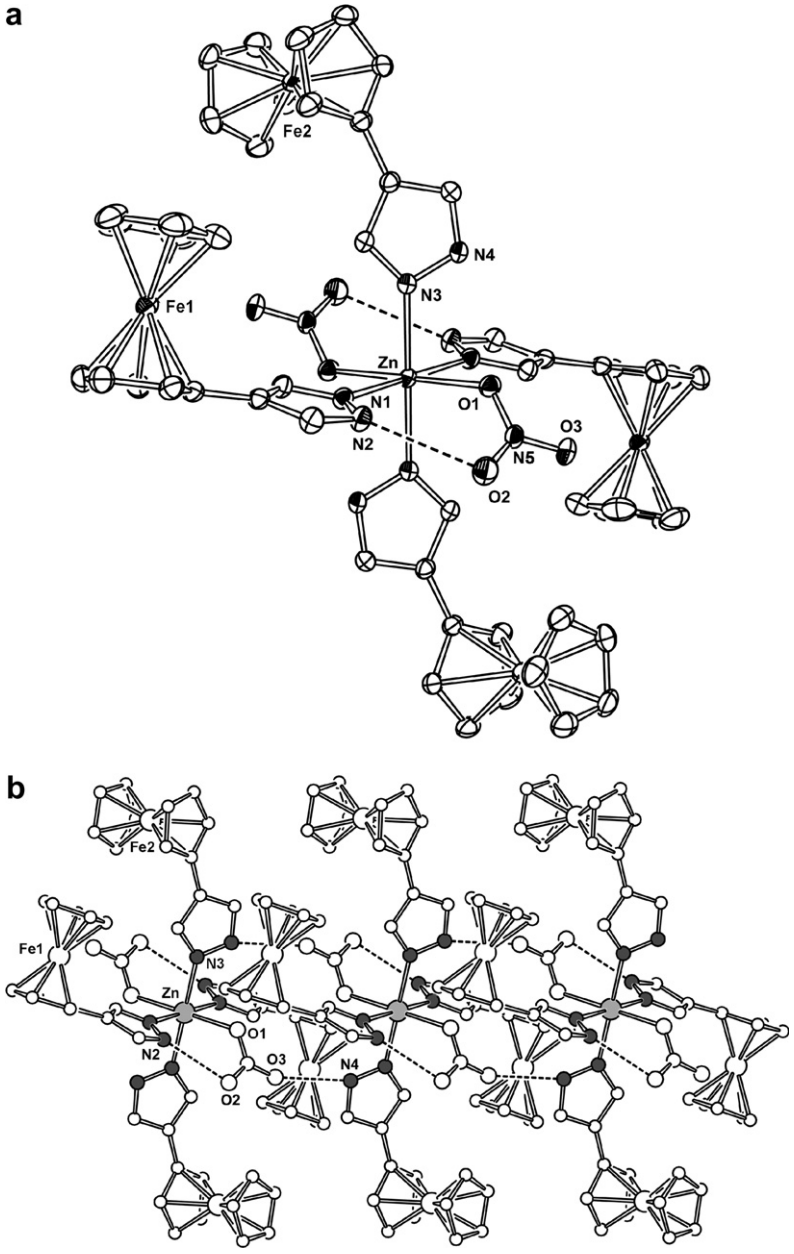

Fig. 5. (a) ORTEP drawing (50% thermal probability ellipsoids) of $[Zn(NO_3)_2(\mathbf{1})_4]$ (**4**) (α-form). (b) Hydrogen-bonded one-dimensional arrangement of **4** in the α-form crystal. Dashed lines indicate hydrogen bonds. Hydrogen atoms are omitted.

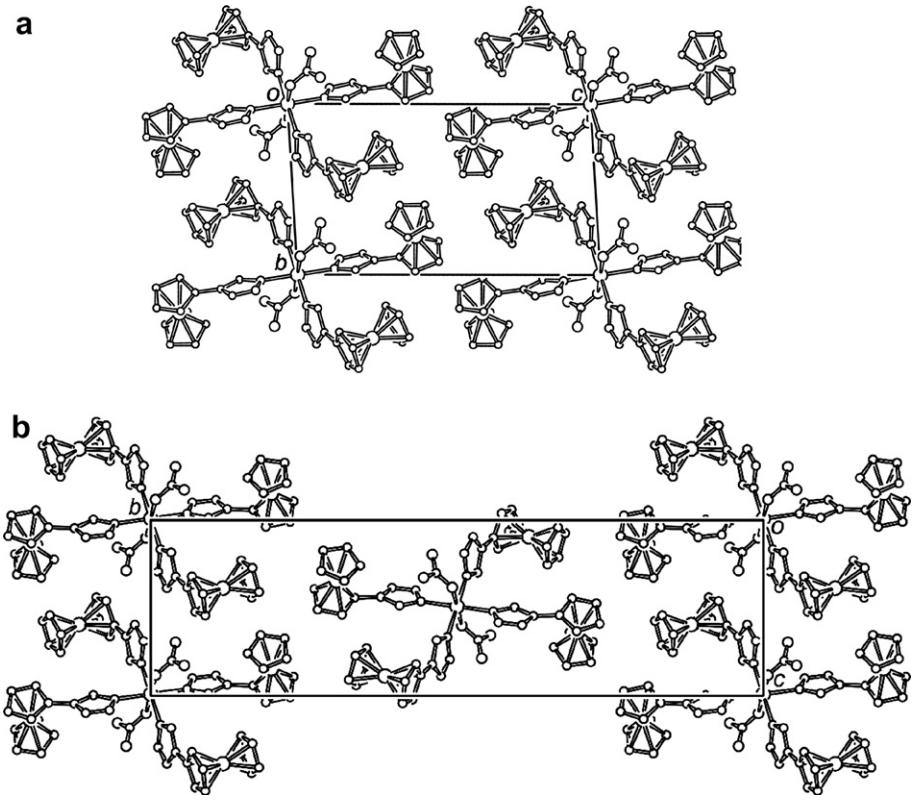

Fig. 6. Packing diagrams of (a) α-form and (b) β-form of $[Zn(NO_3)_2(\mathbf{1})_4]$ (**4**). Hydrogen atoms are omitted.

Packing diagrams of the α- and β-forms, projected along the hydrogen-bonded chain direction, are shown in Fig. 6a and b, respectively. The unit cell volume of the β-form is twice that of the α-form, and in the β-form there is an additional chain at the center of the cell. This polymorphism is attributed to the difference in the arrangement of the supramolecular chains. The calculated densities are comparable (1.619 g cm^{-3} (α-form) and 1.613 g cm^{-3} (β-form)) at room temperature.

$[Co(NO_3)_2(\mathbf{1})_4]$ (**5**) is isostructural with the α-form of **4**. Hydrogen bond lengths are also comparable (Table 3). Reflecting the different ionic radii, the M–N_{FcPz} distance in **5** (2.108(2) Å) is slightly shorter than that in **4** (2.112(1)–2.135(6) Å), and the unit cell volume of **5** is smaller than that of **4**-β by 0.1%. We could not find polymorphs, but considering the structural similarity between **4** and **5**, polymorphism may exist.

The molecular structure of $[CoCl_2(\mathbf{1})_4]$ (**6**) is shown in Fig. 7. The Co ion exhibits an octahedral coordination geometry with the chloride ions at the axial positions. The four NH hydrogens form intramolecular hydrogen bonds with the chlorine atoms, with N···Cl distances of 3.127(2) and 3.085(2) Å. No intermolecular hydrogen bonds are formed.

$[Zn(NCS)_2(\mathbf{1})_2]$ (**7**) was the only example of a trinuclear complex. In the molecule, the Zn ion adopts a tetrahedral coordination environment, coordinated by the nitrogens of two ferrocenyl ligands and two thiocyanate ions. The units form a chain arrangement, as shown in Fig. 8. Intermolecular NH···S hydrogen bonds are formed between the NH group of the ferrocenyl ligand and S(1) of the thiocyanate anion [N···S distance: 3.336(2) Å].

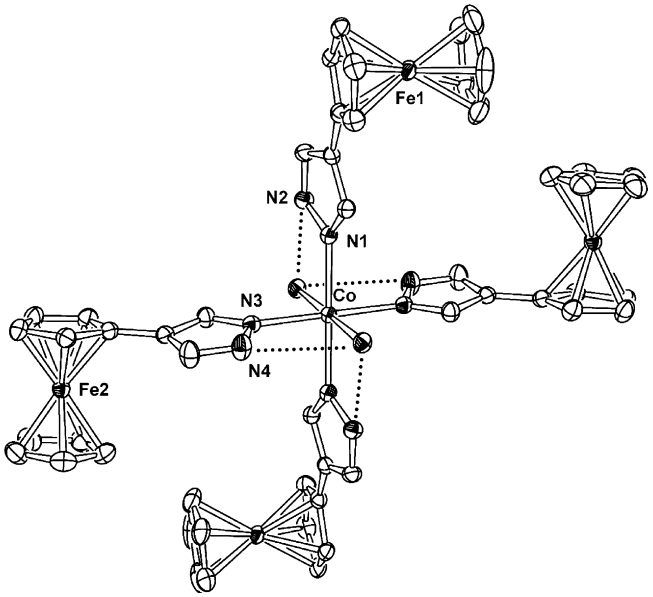

Fig. 7. ORTEP drawing (50% thermal probability ellipsoids) of $[CoCl_2(\mathbf{1})_4]$ (**6**). Dashed lines indicate hydrogen bonds (NH···Cl). Hydrogen atoms are omitted.

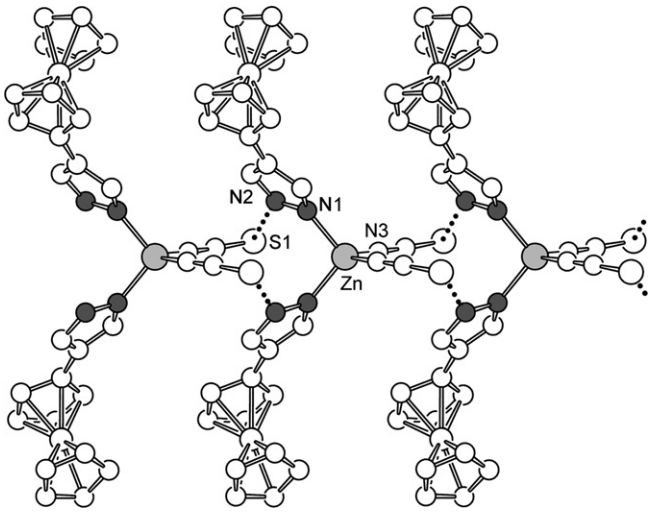

Fig. 8. One-dimensional arrangement of $[Zn(NCS)_2(\mathbf{1})_2]$ (**7**) via weak hydrogen bonding (NH···S) in the crystal. Hydrogen atoms are omitted.

In all of these metal assemblies of **1**, the NH group of the ligand is involved in hydrogen bonding. Coexistence of intramolecular and intermolecular hydrogen bonds was observed in **4** (α-form), **4** (β-form), and **5**, while **6** and **7** exhibited only intramolecular and intermolecular hydrogen bonds, respectively. Similar to **1**, FcPM forms zinc-centered ferrocenyl cluster complexes, $[Zn(NO_3)_2(FcPM)_3]$ and $[Zn(NCS)_2(FcPM)_2]$ [4b], but hydrogen-bond interactions are absent in the FcPM complexes. The stoichiometry and coordination environment of the nitrate complexes are different for FcPM and **1**; the zinc ion is coordinated by three molecules of FcPM and four molecules of **1**, respectively. Flexibility of the coordination environment of zinc ions allows such variation of the L:M ratio [18].

3. Conclusion

We designed the 5-ferrocenylpyrazole ligand (**1**) as a new building block for supramolecular organometallic assembly. The crystal structure of **1** consists of zigzag one-dimensional chains formed via NH···N hydrogen bonds, which is a typical assembly mode for pyrazoles. The ligand has proved useful for construction of supermolecules containing both coordination bonds and hydrogen bonds. The reaction of **1** with metal salts provided metal-centered ferrocenyl clusters, which are further joined via inter-unit hydrogen bonds to form chain structures. Polymorphism, derived from differing arrangements of the chains, was also found.

In the metal complexes under discussion, **1** was used as a neutral ligand. However, pyrazolate anions have been shown to form cyclic metal complexes exhibiting interesting photophysical properties [19]. A study on the synthesis of metal complexes with the pyrazolate anion of **1** is currently in progress in our laboratory, but the desired compounds have not yet been isolated.

4. Experimental

4.1. General

All reagents and solvents were commercially available except for 4-iodo-1-tritylpyrazole [20], which was synthesized by following literature procedures. Solution NMR spectra were recorded on a JEOL JNM-ECL-400 spectrometer. Solid-state NMR spectra were recorded using a Bruker Avance 300 NMR spectrometer with a Bruker MAS 4 mm probe head and a home-built NMR spectrometer with a Tecmag Apollo console, a Doty MAS 7 mm probe head, and an Oxford 7.05 T superconducting magnet system. CP/MAS experiments were performed at 75.43 MHz for ^{13}C with a sample spinning speed of 9 kHz and a CP time of 2 ms. Temperatures of the sample were detected with a thermocouple on the inside near the air inlet of the probe housing, which were corrected with the chemical shift of the carboxyl carbon of samarium acetate [21]. Dipolar dephasing experiments were performed with a dephasing period of 100 μs [22]. ^{13}C spin–lattice relaxation times, T_1, were measured using the method of Torcha [23]. Infrared spectra were recorded on a Shimadzu Prestige-21 FTIR-8400S spectrometer attached with an AIM-8800 microscope in the 4000–400 cm^{-1} range. Cyclic voltammograms were recorded with an ALS/chi electrochemical-analyzer model 600 A in dichloromethane solutions containing 0.1 mol dm^{-3} nBu$_4$NClO$_4$ as the supporting electrolyte, at a scan rate of 0.1 V s^{-1}. An Ag/Ag^+ reference electrode and a glassy carbon disk working electrode were used, and the values were referenced to $(Cp_2Fe)^{+/0}$. Powder X-ray diffraction patterns were recorded on a MAC Science M03XHF22 diffractometer. DSC measurements were performed using a Q100 differential scanning calorimeter (TA instruments) in the temperature range 100–460 K at a rate of 10 K min^{-1}. Thermogravimetric (TG) analysis was performed under a nitrogen atmosphere at a heating rate 10 K min^{-1} on a Seiko TG/DTA 220U, in the temperature range 25–400 °C.

4.2. 4-Ferrocenyl-1-pyrazole (*1*)

4-Ferrocenyl-1-tritylpyrazole (**2**, see below) (1.80 g, 3.63 mmol) was dissolved in a mixture of dichloromethane and methanol (1:1 v/v, 80 mL), to which acetic acid (12 mL) was added. The solution was refluxed for about 1 week. After removal of the solvent under reduced pressure, the residue was dissolved in dichloromethane (80 mL), and washed with an aqueous solution of sodium bicarbonate (5 g, 60 mL) and water (80 mL × 3). The organic layer was separated, dried with magnesium sulfate, and the solvent was removed under reduced pressure. The crude product was purified by column chromatography (silica gel, eluent chloroform:acetone = 8:2). The second band ($R_f = 0.25$) gave 4-ferrocenyl-1-pyrazole (**1**) as fine needle crystals (0.87 g, yield 95%). The compound was recrystallized from hexane and acetonitrile. UV–Vis

(MeCN, λ/nm, ε): 207 (19796), 219 (19484), 270 (5532), 341 (101), 452 (214); IR (cm^{-1}): 3118s, 2934s, 1370m, 1147m, 1105m, 1012s, 957m, 865s, 802s, 3103s, 2949s, 1728m, 1597m, 1371s, 1317m, 1140m, 1105s, 1022s, 866s; ^1H NMR (400 MHz, $CDCl_3$): δ 4.05 (s, 5H), 4.22 (t, 2H, $J = 1.8$ Hz), 4.45 (t, 2H, $J = 1.8$ Hz), 7.63 (s, 2H); ^1H NMR (400 MHz, DMSO-d_6): δ 3.99 (s, 5H), 4.18 (t, 2H, $J = 1.8$ Hz), 4.52 (t, 2H, $J = 1.8$ Hz), 7.61 (s, 1H), 7.81 (s, 1H), 12.67 (br, 1H). Anal. Calc. for $C_{13}H_{12}FeN_2$: C, 61.94; H, 4.80; N, 11.11. Found: C, 61.83; H, 4.82, N, 11.22%. Orange plate crystals of **1** suitable for X-ray analysis were obtained by slow cooling of a hot acetonitrile solution of **1**. Crystals of the chloroform solvate, $\mathbf{1} \cdot 0.5CHCl_3$, were obtained by slow evaporation of a dichloromethane solution of **1**. Crystals from hexane, confirmed to be in the non-solvated form by powder X-ray diffraction, were used for calorimetric studies.

4.3. 4-Ferrocenyl-1-tritylpyrazole (2)

Under a nitrogen atmosphere, *tert*-butyllithium (11 mL, 16.0 mmol; 1.45 M in *n*-pentane) and a THF suspension (22 mL) of zinc chloride (2.43 g, 17.8 mmol) were successively added slowly to a THF (11 mL) solution of ferrocene (2.35 g, 12.6 mmol) cooled in an ice bath. The solution was allowed to warm to room temperature, and stirred for 1 h. To this solution, a THF suspension (12 mL) of bis(triphenylphosphine)palladium chloride (0.455 g) and a THF solution (30 mL) of 4-iodo-1-tritylpyrazole (5.479 g, 12.6 mmol) were added successively. After stirring the solution at room temperature for 1 day, water (5 mL) was added, and insoluble materials were removed by filtration. The filtrate was concentrated, and the residue was extracted with diethyl ether (250 mL). The organic layer was washed with water (150 mL × 4) and brine (100 mL), and dried with magnesium sulfate. After removing the solvent under reduced pressure, the residue was purified by column chromatography (silica gel, eluent dichloromethane:hexane = 7:3). The first band gave ferrocene, and the second band ($R_f = 0.25$) gave the desired product as brown powders (3.44 g, yield 55%). ^1H NMR (400 MHz, $CDCl_3$): δ 3.99 (s, 5H), 4.16 (t, 2H), 4.37 (t, 2H), 7.18–7.20 (m, 6H), 7.31–7.34 (m, 10H), 7.71 (s, 1H). The product was further used for the preparation of **1**. Orange plate crystals of **2** suitable for X-ray analysis were obtained by recrystallization from acetonitrile.

4.4. 4-Ferrocenyl-1-methylpyrazole (3)

Under a nitrogen atmosphere, sodium hydride (107 mg, 2.23–3.21 mmol; 50–72% in oil) was dispersed in THF (20 mL), to which **1** (60 mg, 0.23 mmol) was added slowly under stirring. After the evolution of hydrogen ceased, methyl iodide (1 mL) was added to this solution, and stirring continued overnight at room temperature. The solvent was removed under reduced pressure, and the residue was dissolved in dichloromethane and washed with water. The organic layer was dried over magnesium sulfate and then evaporated. The crude product was recrystallized from hexane. Yellow powder (31 mg, 49%). ^1H NMR (400 MHz, $CDCl_3$): δ 3.89 (s, 3H), 4.04 (s, 5H), 4.20 (t, 2H, $J = 1.8$ Hz), 4.41 (t, 2H, $J = 1.8$ Hz), 7.35 (s, 1H), 7.54 (s, 1H). Anal. Calc. for $C_{14}H_{14}FeN_2$: C, 63.19; H, 5.30; N, 10.53. Found: C, 63.15; H, 5.40; N, 10.72%. Orange prismatic crystals of **3** suitable for X-ray analysis were obtained by recrystallization from acetone.

4.5. [Zn(NO3)2(1)4] (4)

Methanol solutions (0.5 mL) of **1** (3 mg, 1.2×10^{-2} mmol) and $Zn(NO_3)_2 \cdot 6H_2O$ (3.9 mg, 1.19×10^{-2} mmol) were mixed and left to stand at room temperature. Orange plate crystals were formed in a week. The results of elemental analysis indicated that a 1:3 M/L complex was the major product. Anal. Calc. for $C_{39}H_{36}ZnFe_3N_8O_6$ [$=Zn(NO_3)_2(\mathbf{1})_3$]: C, 48.61; H, 3.97; N, 11.63. Found: C, 48.71; H, 4.03; N, 11.65%.

4.6. [Co(NO3)2(1)4] (5)

This complex was prepared as described for **4**, using $Co(NO_3)_2 \cdot 3H_2O$ and acetonitrile as a solvent. Orange plate crystals were obtained. Anal. Calc. for $C_{52}H_{48}Cl_2CoFe_4N_8$: C, 52.43; H, 4.06; N, 11.76. Found: C, 52.19; H, 4.11; N, 11.86%.

4.7. [CoCl2(1)4] (6)

This complex was prepared as described for **4**, using $CoCl_2 \cdot 6H_2O$ and ethanol as a solvent. Orange plate crystals were obtained. Elemental analysis indicated that a 1:3 M/L complex was the major product. Anal. Calc. for $C_{39}H_{36}Cl_2CoFe_3N_6$ [$=CoCl_2(\mathbf{1})_3$]: C, 51.81; H, 4.24; N, 9.30. Found: C, 51.75; H, 4.36, N, 9.53%.

4.8. [Zn(NCS)2(1)2] (7)

This complex was prepared as described for **4**, using $Zn(SCN)_2$ and methanol as a solvent. Orange plate crystals were obtained. Anal. Calc. for $C_{28}H_{24}Fe_2N_6S_2Zn$: C, 49.04; H, 3.53; N, 12.26. Found: C, 48.66; H, 3.64; N, 11.96%.

4.9. cis-[Pt(NH3)2(1)2](PF6)2 (8)

cis-$[PtCl_2(NH_3)_2]$ (18 mg, 0.060 mmol) and $AgPF_6$ (33 mg, 0.131 mmol) were dissolved in water (4 mL). The solution was heated at 60 °C for 3 h in the absence of light, and then filtered through Celite and added to a methanol solution (2 mL) of **1** (30 mg, 0.12 mmol). After stirring at room temperature for 1 day in the absence of light, the solvent was removed under reduced pressure, giving a yellow-brown powder (58 mg, 94%). The reaction afforded the desired product almost quantitatively, and no by-products

were observed. UV–Vis (MeCN, λ/nm, ε): 223 (28 259), 264 (15 216), 433 (948), 849 (17 538). ^{1}H NMR (DMSO-d_6, ppm): δ 4.03 (s, 10H), 4.26 (s, 4H), 4.56 (s, 4H), 4.70 (br, 6H), 7.94 (s, 2H), 8.29 (s, 2H), 13.93 (s, 2H). Anal. Calc. for $C_{26}H_{30}N_6F_{12}P_2Fe_2Pt$: C, 30.52; H, 2.96; N, 8.21%. Found: C, 29.87; H, 3.10; N, 8.00%.

4.10. *trans*-[Pt(NH$_3$)$_2$(**1**)$_4$](PF$_6$)$_2$ (**9**)

trans-[$PtCl_2(NH_3)_2$] (31 mg, 0.103 mmol) and $AgPF_6$ (53 mg, 0.208 mmol) were dissolved in water (4 mL). The solution was heated at 60 °C for 3 h in the absence of light, and then filtered through Celite and added to a methanol

Table 5
Crystallographic data for **1**–**3**

	1	**1** · 0.5$CHCl_3$	**2**	**3**
Empirical formula	$C_{13}H_{12}FeN_2$	$C_{27}H_{25}Fe_2Cl_3N_4$	$C_{32}H_{26}FeN_2$	$C_{14}H_{14}FeN_2$
Formula weight	252.10	623.56	494.40	266.12
Crystal system	Triclinic	Triclinic	Triclinic	Orthorhombic
Space group	$P\bar{1}$	$P\bar{1}$	$P\bar{1}$	$P2_12_12_1$
a (Å)	7.4330(8)	7.456(2)	9.4982(7)	5.7993(4)
b (Å)	9.9266(1)	10.498(3)	12.382(1)	12.0445(9)
c (Å)	15.9111(2)	16.990(5)	12.438(1)	16.5028(1)
α (°)	80.061(2)	76.308(5)	112.971(2)	
β (°)	87.867(2)	89.620(5)	106.583(2)	
γ (°)	69.978(2)	88.498(5)	103.675(2)	
V (Å^3)	1086.2(2)	1291.6(6)	1186.3(2)	1152.71(2)
Z	4	2	2	4
d_{calc} (g cm^{-3})	1.542	1.603	1.384	1.533
T (K)	173	120	296	173
μ (cm^{-1})	1.357	1.46	0.66	1.284
Reflections collected	7913	9042	9015	8602
Independent reflections	5294	6344	5873	2854
Parameters	305	325	342	190
R_1[a], wR_2[b] ($I > 2\sigma$)	0.0354; 0.0787	0.0593; 0.1179	0.0627; 0.1254	0.0338; 0.0776
R_1[a], wR_2[b] (all data)	0.0443; 0.0828	0.1586; 0.1455	0.1315; 0.1489	0.0375; 0.0793
Goodness-of-fit	1.011	1.019	1.019	1.047

[a] $R_1 = \sum||F_o| - |F_c||/\sum|F_o|$.
[b] $wR_2 = \left[\sum w(F_o^2 - F_c^2)^2/\sum w(F_o^2)^2\right]^{1/2}$.

Table 6
Crystallographic data for **4**–**7**

	4 (α-form)	**4** (β-form)	**5**	**6**	**7**
Empirical formula	$C_{52}H_{48}Fe_4N_{10}O_6Zn$	$C_{52}H_{48}Fe_4N_{10}O_6Zn$	$C_{52}H_{48}CoFe_4N_{10}O_6$	$C_{52}H_{48}Cl_2CoFe_4N_8$	$C_{28}H_{24}Fe_2N_6S_2Zn$
Formula weight	1197.77	1197.79	1191.33	1138.21	685.72
Crystal system	Triclinic	Monoclinic	Triclinic	Monoclinic	Monoclinic
Space group	$P\bar{1}$	$P2_1/c$	$P\bar{1}$	$C2/c$	$P2/c$
a (Å)	7.5127(4)	7.5111(8)	7.5230(7)	35.881(3)	16.715(2)
b (Å)	9.6742(6)	34.097(3)	9.6502(1)	9.6608(8)	6.2461(9)
c (Å)	16.9404(1)	11.3874(9)	16.9190(2)	14.2771(1)	14.421(2)
α (°)	85.3640(1)		85.462(2)		
β (°)	83.0270(1)	122.250(5)	82.978(2)	109.377(2)	98.464(3)
γ (°)	79.6820(1)		79.998(2)		
V (Å^3)	1200.15(1)	2466.5(4)	1198.4(2)	4668.7(7)	1386.0(3)
Z	1	2	1	4	2
d_{calc} (g cm^{-3})	1.657	1.613	1.651	1.723	1.643
T (K)	173	293	173	173	293
μ (cm^{-1})	1.736	1.690	1.584	1.723	2.072
Reflections collected	8939	17 672	8934	16 839	9803
Independent reflections	5867	6097	5856	5771	3442
Parameters	427	331	339	304	177
R_1[a], wR_2[b] ($I > 2\sigma$)	0.0251; 0.0628	0.0876; 0.2071	0.0379; 0.0782	0.0363; 0.0776	0.0338; 0.0901
R_1[a], wR_2[b] (all data)	0.0279; 0.0725	0.1005; 0.2189	0.0567; 0.0859	0.0485; 0.0826	0.0442; 0.0962
Goodness-of-fit	1.008	1.033	0.998	1.004	1.028

[a] $R_1 = \sum||F_o| - |F_c||/\sum|F_o|$.
[b] $wR_2 = \left[\sum w(F_o^2 - F_c^2)^2/\sum w(F_o^2)^2\right]^{1/2}$.

solution (3 mL) of **1** (53 mg, 0.210 mmol). After stirring at 45 °C for 17 h in the absence of light, the solvent was removed under reduced pressure. The product was dissolved in acetone, filtered through Celite, and concentrated; chloroform was added to the concentrate, and the solution was cooled in a refrigerator. A yellow-brown powder was obtained (72 mg, 68%). The sample was purified by recrystallization from acetone/chloroform. UV–Vis (MeCN, λ/nm, ε): 227 (27132), 267 (16284), 445 (511), 849 (38). ^{1}H NMR (DMSO-d_6, ppm): δ 4.11 (s, 10H), 4.31 (s, 4H), 4.51 (br, 6H), 4.62 (s, 4H), 8.07 (s, 2H), 8.38 (s, 2H), 14.21 (s, 2H). Anal. Calc. for $C_{26}H_{30}N_6F_{12}P_2Fe_2Pt$: C, 30.52; H, 2.96; N, 8.21. Found: C, 29.87; H, 3.10; N, 8.00%.

4.11. X-ray crystallography

X-ray diffraction data for single crystals were collected on a Bruker SMART APEX CCD diffractometer, using Mo Kα radiation ($\lambda = 0.71073$ Å). Crystal data, data collection parameters, and analysis statistics for these compounds are listed in Tables 5 and 6. All calculations were performed using the crystallographic software packages of SHELXL [24]. The data were corrected for absorption using the SADABS program [25]. The structure was solved by the direct method (SHELXS 97) and expanded using Fourier techniques. The non-hydrogen atoms were refined anisotropically. NH hydrogens were located from the Fourier map, and other hydrogen atoms were inserted at the calculated positions and allowed to ride on their respective parent atoms. Molecular graphics were drawn using ORTEP-3 for Windows [26].

Acknowledgements

This work was financially supported by a Grant-in-Aid for Scientific Research (No. 17685003) from the JSPS (Japan Society for the Promotion of Science) and by the "High-Tech Research Center" Project 2005–2009 of MEXT (Ministry of Education, Culture, Sports, Science and Technology). We thank Takahiro Akasaka (Toho University) for X-ray crystallography and Hideaki Nakamura (The University of Electro-Communications) for analysis of NMR data. We also thank Masaru Nakama (WarpStream, Inc., Tokyo) for providing Web-based database systems. NMR experiments were partly carried out at Hosei University Research Center for Micro-Nano Technology. We thank Professor H. Ogata (Hosei University) for use of the Bruker Avance 300 NMR spectrometer.

Appendix A. Supplementary material

CCDC 618689, 618690, 618691, 618708, 618694, 618695, 618693, 618692 and 61896 contain the supplementary crystallographic data for **1**, **1** · $CHCl_3$, **2**, **3**, **4**, (α-form), **4**, (β-form), **5**, **6** and **7**. The data can be obtained free of charge via htpp://www.ccdc.cam.ac.uk/conts/retrieving.html, or from the Cambridge Crystallographic Data Centre, 12 Union Road, Cambridge CB2 1EZ, UK; fax: (+44) 1223-336-033; or e-mail: deposit@ccdc.cam.ac.uk.

References

[1] (a) I. Haiduc, F.T. Edelmann, Supramolecular Organometallic Chemistry, Wiley-VCH, Weinheim, 1999;
(b) J.W. Steed, J.L. Atwood, Supramolecular Chemistry, Wiely & Sons, Chichester, 2000;
(c) M. Oh, G.B. Carpenter, D.A. Sweigart, Acc. Chem. Res. 27 (2004) 1.

[2] (a) J.-M. Lehn, J.L. Atwood, J.E.D. Davis, D.D. MacNicol, F. Vögtle (Eds.), Comprehensive Supramolecular Chemistry, Vols. 1–11, Pergamon Press, Oxford, 1990;
(b) J.-M. Lehn, Supramolecular Chemistry, Concepts and Perspectives, VCH, Weinheim, 1995.

[3] (a) D. Braga, F. Grepioni, G.R. Desiraju, Chem. Rev. 98 (1998) 1375;
(b) D. Braga, L. Maini, M. Polito, L. Scaccianoce, G. Cojazzi, F. Grepioni, Coord. Chem. Rev. 216–217 (2002) 225.

[4] (a) R. Horikoshi, C. Nambu, T. Mochida, Inorg. Chem. 42 (2003) 6868;
(b) R. Horikoshi, K. Okazawa, T. Mochida, J. Organomet. Chem. 690 (2005) 1793;
(c) R. Horikoshi, M. Ueda, T. Mochida, New J. Chem. 27 (2003) 933;
(d) R. Horikoshi, C. Nambu, T. Mochida, New J. Chem. 28 (2004) 26;
(e) T. Mochida, H. Shimizu, K. Okazawa, Inorg. Chim. Acta, in press.

[5] (a) R. Horikoshi, T. Mochida, H. Moriyama, Inorg. Chem. 41 (2002) 3017;
(b) R. Horikoshi, T. Mochida, R. Torigoe, Y. Yamamoto, Eur. J. Inorg. Chem. (2002) 3197;
(c) T. Mochida, K. Okazawa, R. Horikoshi, Dalton Trans. (2006) 693.

[6] T. Mochida, H. Shimizu, S. Suzuki, T. Akasaka, J. Organomet. Chem. 691 (2006) 4882.

[7] L. Infantes, C. Foces-Foces, J. Elguero, Acta Crystallogr., Sect. B 55 (1999) 441, and references cited therein.

[8] O. Klein, F. Aguilar-Parrilla, J.M. Lopez, N. Jagerovic, J. Elguero, H.-H. Limbach, J. Am. Chem. Soc. 126 (2004) 11718, and references cited therein.

[9] (a) A.P. Sadimenko, S.S. Basson, Coord. Chem. Rev. 147 (1996) 247;
(b) S. Trofimenko, Chem. Rev. 72 (1972) 497;
(c) F. Bonati, Chim. l'Ind. (Italy) 62 (1980) 323.

[10] (a) K. Niedenzu, J. Serwatowski, S. Trofimenko, Inorg. Chem. 30 (1991) 524;
(b) J.A. Campo, M. Cano, J.V. Heras, E. Pinilla, M. Ruiz-Bermejo, R. Torres, J. Organomet. Chem. 582 (1999) 173;
(c) L.-F. Tang, W.-L. Jia, Z.-H. Wang, J.-F. Chai, J.-T. Wang, J. Organomet. Chem. 637–639 (2001) 209.

[11] (a) E.M. Barranco, M.C. Gimeno, A. Laguna, M.D. Villacampa, Inorg. Chim. Acta 358 (2005) 4177;
(b) X.-X. Gan, R.-Y. Tan, H.-B. Song, X.-M. Zhao, L.-F. Tang, J. Coord. Chem. 59 (2006) 783.

[12] (a) D. Braga, M. Polito, S.L. Giaffreda, F. Grepioni, Fabrizia. Dalton Trans. (2005) 2766;
(b) E.M. Barranco, O. Crespo, M.C. Gimeno, P.G. Jones, A. Laguna, Eur. J. Inorg. Chem. (2004) 4820;
(c) G. Li, Y. Song, H. Hou, L. Li, Y. Fan, Y. Zhu, X. Meng, L. Mi, Inorg. Chem. 42 (2003) 913.

[13] E. Negishi (Ed.), Handbook of Organopalladium Chemistry for Organic Synthesis, Wiley-Interscience, New York, 2002.

[14] C.W. Fong, Aust. J. Chem. 33 (1980) 1763.

[15] (a) O. Carugo, G.D. Santis, L. Fabbrizzi, M. Licchelli, A. Monichino, R. Rallavicini, Inorg. Chem. 31 (1992) 765;
(b) J. Rajput, J.R. Moss, A.T. Hutton, D.T. Hendricks, G.E. Arendse, C. Imrie, J. Organomet. Chem. 689 (2004) 1553;
(c) E.M. Barranco, O. Cresspo, M.C. Gimeno, P.G. Jones, A. Laguna, M.D. Villacampa, J. Organomet. Chem. 592 (1999) 258.
[16] (a) R.M. Claramunt, M.D.S. María, I. Forfar, F. Aguilar-Parrilla, M. Minguet-Bonvehí, O. Klein, H.-H. Limbach, C. Foces-Foces, A.L. Llamas-Saiz, J. Elguero, J. Chem. Soc., Perkin Trans. 2 (1997) 1867;
(b) P. Cabildo, R.M. Claramunt, I. Forfar, C. Foces-Foces, A.L. Llamas-Saiz, J. Elguero, Heterocycles 37 (1994) 1623.
[17] (a) A.D. Davydov, Solitons in Molecular Systems, Reidel, Dordecht, Holland, 1985;
(b) T. Bountis (Ed.), Proton Transfer in Hydrogen-Bonded Systems, Plenum Press, New York, 1992;
(c) M. Szafrański, A. Katrusiak, G.J. McIntyre, Phys. Rev. Lett. 89 (2002) 215507.
[18] A. Erxleben, Coord. Chem. Rev. 246 (2003) 203.
[19] (a) H.V.R. Dias, H.V.K. Diyabalanage, M.G. Eldabaja, O. Elbjeirami, M.A. Rawashdeh-Omary, M.A. Ommary, J. Am. Chem. Soc. 127 (2005) 7489;
(b) G. Mezei, R.G. Raptis, Inorg. Chim. Acta 358 (2004) 3279.
[20] J. Elguero, C. Jaramillo, C. Pardo, Synthesis (1997) 563.
[21] G.C. Campbell, R.C. Crosby, J.F. Haw, J. Magn. Reson. 69 (1986) 191.
[22] S.J. Opella, M.H. Frey, J. Am. Chem. Soc. 101 (1979) 5854.
[23] D.A. Torchia, J. Magn. Reson. 30 (1978) 613.
[24] G.M. Sheldrick, SHELXL: Program for the Solution for Crystal Structures, University of Göttingen, Germany, 1997.
[25] G.M. Sheldrick, SADABS: Program for Semi-empirical Absorption Correction, University of Göttingen, Germany, 1997.
[26] ORTEP-3 for Windows: L.J. Farrugia, J. Appl. Crystallogr. 30 (1997) 565.